

Mixed algorithmic-analog simulation of many body dynamics using interaction of fixed-frequency superconducting qubits

D. V. Babukhin^{1,2}, A. A. Zhukov^{1,3}, W. V. Pogosov^{1,4}

¹*Dukhov Research Institute of Automatics (VNIIA), 127055 Moscow, Russia*

²*Russian Quantum Center (RQC), 143026 Moscow, Russia*

³*National Research Nuclear University (MEPhI), 115409 Moscow, Russia and*

⁴*Institute for Theoretical and Applied Electrodynamics,
Russian Academy of Sciences, 125412 Moscow, Russia*

In recent years there was a huge experimental progress towards the development of prototypes of algorithmic quantum processors. These quantum machines are not free from imperfections and various technological and scientific problems remain to be solved in the following years. Until that moment computational schemes different from the digital approach can be used in order to perform calculations using state-of-the-art quantum hardware. A prospective idea is to combine positive aspects of both digital and analog computation. Particularly, it is possible to use qubit-qubit interaction embedded in architecture in order to replace those parts of algorithms which are responsible for the quantum entanglement. In this paper, we provide an example of such an approach based on unwanted couplings between fixed-frequency superconducting qubits (crosstalks). These couplings are normally considered as a source of errors in standard digital quantum computation, but we argue that they can be utilized instead of two-qubit gates in some quantum algorithms thus avoiding an accumulation of errors associated with these gates. We illustrate our ideas with quantum processors of IBM Quantum Experience, which are used by us for simulating the dynamics of spin clusters through the Trotterized evolution. We demonstrate a significant improvement in the quality of results compared to the conventional digital approach with the same processor. We also show that crosstalks result in a highly non-markovian dynamics of qubits. This fact must be taken into account while developing error-correction strategies with qubits of this type.

PACS numbers:

I. INTRODUCTION

Quantum computation is a computing paradigm, emerged at the end of the 20th century in the works of Manin [1] and Feynmann [2]. This approach to computing is interesting in many ways, the most intriguing that it promises a quantum speed-up in some important problems like prime number factorization [3], solving a system of linear equations [4], quantum principal component analysis [5] and many others. This speed-up provided with quantum computing to many practically important problems was referred to as "quantum supremacy" [6] and it is a holy grail of nowadays quantum computing science to build quantum processors able to attain it.

During a last couple of decades there was a huge progress in the field of experimental quantum computing. It led to the point, when first prototypes of quantum processors became available [7–9]. These imperfect realizations of quantum computing devices are gathered under the term NISQ, which is noisy intermediate scale quantum devices [10]. This class of processing units is characterized by imperfect implementation of single-qubit and two-qubit gates, which are important to provide a universal set of gates for computation, imperfect readout of qubit quantum states and limited connectivity between qubits. Unavoidable imperfections of physical hardware (which are present both for classical and quantum computation) require development of error correction techniques. In principle, all errors which occur during computation, can be eliminated using error correction codes. For quantum computation there were developed various error correction codes in the last 20 years (see, e.g., Refs. [11, 12]). Nevertheless, it is currently impossible to effectively use those methods in order to obtain any practical improvement due to various imperfections of quantum hardware, and other methods of error mitigation are being developed [13–16]. Yet there is a plenty of works done to date, which utilizes the existing imperfect processors to solve interesting problems, serving as a playground for future industry-level applications (see, for example, Refs. [17, 18]).

One of the main applications of quantum computation is effective calculation of properties of many-body quantum systems. Those systems are described by wave functions residing in a Hilbert space, whose dimensionality grows exponentially with the number of particles in a system, making it practically intractable for classical calculations

from first principles even for a modest system size. With quantum computing, it becomes possible to operate with exponentially-many quantum states at a time (due to superposition principle) with linear number of quantum gates. Having a properly defined observable, a huge speed-up of computation can be obtained this way.

Modelling many body quantum systems usually requires to apply multiple two-qubit gates to a register of qubits in order to create a highly-entangled state or to model system's temporal dynamics. To date, two-qubit gates are the most noisy part of quantum hardware, and as many those gates were used, as higher will be errors. So until the quality of those gates reaches an appropriate limit it is reasonable to consider alternative strategies to perform quantum computation with existing devices without relying totally on gate model.

A possible way to proceed under these circumstances is to consider alternative approaches to quantum computation. Historically there were two main approaches known as algorithmic (digital) quantum computation and analog quantum computation. Algorithmic approach is based on a canonical quantum gate model, every quantum program is in essence a sequence of gates from a universal set, which realize some transformation of a state of register qubits. In order to use such an approach there must be control operations on qubits states of a very high precision. The analog approach uses a quantum system with controllable dynamics, which is able to mimic dynamics of another system. In this approach one does not use any gate for computation, all that needed is to prepare a simulator system and to let it evolve for some time.

Among these flavors of quantum computation it is possible to rely on a mixed strategy, which can collect the best of the two worlds. In essence, a register of qubits is being controlled with individual qubit operations from one side, and with evolution under a Hamiltonian, embedded in quantum hardware on a physical level, from another side. This approach can be useful for problems where a fixed entangler is required to create an initial entangled state and then measure some observables, e.g., a variational quantum computation approach, which showed several successful applications in recent years [17, 18]. It also possibly has an even greater potential in the field of modelling of many body systems [19], e.g., emulation of many body localization with superconducting qubits [23, 24] and ions [25], or investigating entanglement propagation between qubits [26]. For example, in [23] a programmable quantum simulator was used to observe many body localization effect in XY model with all-to-all interactions. This simulator consists of superconducting qubits with tunable frequencies, connected to a resonator, which provides an interaction between qubits through intermediate virtual photons. Each qubit frequency and qubit state can be controlled individually. Such a quantum hardware provides a wide range of opportunities to investigate properties of interacting spin systems. Furthermore, using such an approach it is also possible to accomplish basic subroutines of quantum computation like quantum Fourier transform [27].

In this paper we provide another example on the mixed simulation approach by using a rather unexpected feature of superconducting quantum processors with fixed frequency qubits. Our approach relies on residual interactions (couplings) between fixed frequency qubits connected by resonators, which are known as crosstalks. We illustrate our ideas with superconducting quantum processors of IBM Quantum Experience. Basically, the crosstalks are responsible for additional errors in canonical digital quantum computation. In contrast, we here use them to simulate many body systems with Hamiltonians having interaction terms similar to these couplings. Within this approach we avoid execution of two-qubit quantum gates, thus reducing error accumulation. Our results for the dynamics of 14-spin transverse-field Ising cluster under several Trotter steps are much more accurate than the results of a similar computation based on standard CNOT gates with the same quantum processor. We stress that these results are obtained with the available quantum processor where crosstalks are intentionally suppressed, but in principle a hardware can be optimized in another way, i.e., to improve a quality of such a mixed quantum computation based on crosstalks (keeping individual addressability of qubits).

We also provide a simple experiment to show that the residual qubit-qubit interaction adds a highly non-markovian dynamics to the temporal evolution of quantum states of the chip. Such an evolution is important to take into account while developing error-correction strategies with quantum error correcting codes. Note also that the approach we here consider can be exploited for variational quantum computations with the "natural" entangler.

II. SUPERCONDUCTING FIXED-FREQUENCY QUBITS AND THE ORIGIN OF THEIR RESIDUAL INTERACTION

Nowadays there are several realizations of algorithmic quantum computers available for experiments and benchmarking of quantum computing ideas [7–9]. Superconducting technology was the first one to become a massively available

tool and by now there are numerous papers dealing with the implementation of both known and new algorithms. In our work we concentrate on quantum processors with fixed-frequency qubits.

Quantum processors of this type are built on transmon qubits [29]. A transmon is a superconducting qubit consisting of a Josephson junction shunted by large capacitor. The resonance frequency of these devices is typically in the range of 4-6 GHz. In terms of a lumped circuit model it is well described with a parallel LC oscillator with the inductor L_J being nonlinear and a capacitor C_Σ being linear. The qubit itself is built on two levels of the resulting anharmonic oscillator, and for selective control of its transitions and effective separation of the qubit Hilbert space a sufficiently large anharmonicity is required. In this architecture, qubits frequencies are fixed which enables to have long coherence times. Full single qubit control is accomplished by applying external microwave driving through a transmission line strongly coupled to qubits. Some qubits are coupled through resonators with frequency far away from frequency of every qubit that corresponds to a dispersive regime. This allows to do measurements of qubits states as well as to apply two-qubit gates.

In general, qubits coupled by resonator interact with each other via virtual photons (even in absence of controlling pulses) this interacting being described by Dicke model. Since the frequency of the photon is significantly larger than the excitation frequencies of qubits, photons can be eliminated from the effective description of the system using, e.g., perturbation theory. The latter results in the interaction between those qubits which are coupled by resonator. Thus, the degrees of freedom related to physical qubits slightly hybridize with each other.

In order to keep an individual addressability of qubits in the view of the hybridization, a modified set of two level systems can be introduced which lead to the diagonalization of the Hamiltonian in the new basis. These new qubits, which actually form computational basis, are constructed from the degrees of freedom of transmons with small contributions from the degrees of freedom of other transmons connected with the given one through resonators. However, transmons cannot be treated as ideal two-level systems due to limited anharmonicity. Higher levels of transmons can be populated via transitions from the first excited state. The incorporation of higher levels into the effective description results in the additional interaction of Ising ZZ type in the Hamiltonian of qubits in the computational basis [29]. The interaction between two qubits 1 and 2 in the computational basis connected by the resonator is given by the term of the form $-J_{1,2}^{phys} \sigma_1^z \sigma_2^z$, where $J_{1,2}^{phys} \sim (\delta_1 + \delta_2)$, $\delta_{1,2}$ being anharmonicities of qubits 1 and 2; $J_{1,2}^{phys}$ also depends on detunings between various frequencies [30].

For a quantum processor build from fixed-frequency qubits, a connectivity map of qubit-qubit interaction coincides with the connectivity map of two-qubit gates of the processor. Let us stress that this interaction is static and exists even when gates are not active. The values of J_{ij}^{phys} between different qubits are provided for all quantum devices of IBM Quantum Experience project [31] and typical J_{ij}^{phys} is nearly 50-100 kHz all of them being positive. Thus, $1/J_{ij}^{phys}$ is usually nearly several times smaller than both T_1 and T_2 , which implies that it is possible to perform few entangling operations using embedded ZZ interaction before the decoherence would play a significant role. For example, for 5-qubit chip IBM QX2 $\overline{J_{ij}^{phys} T_1} \approx 4.3$ and $\overline{J_{ij}^{phys} T_2} \approx 3.8$, where averaging is performed over all qubits of the device. For 14-qubit chip IBM QX14 $\overline{J_{ij}^{phys} T_1} \approx 2.6$ and $\overline{J_{ij}^{phys} T_2} \approx 3.6$.

Notice that all these estimates are made for the available quantum hardware, which is optimized to keep crosstalks minimum. We believe that it is possible to optimize hardware in such a way as to improve further these estimates, i.e., to increase typical values of $J_{ij}^{phys} T_{1,2}$ and to enable for the larger numbers of entangling steps of the algorithm. Of course, this also implies a trade-off between the individual addressability of qubits and increase of crosstalks.

Strictly speaking, effective Hamiltonian for fixed-frequency qubits contains not only additional terms of ZZ type, but also terms of other sorts (such as ZX), which are, however, subdominant within a perturbative expansion [30]. If we disregard them in our computation scheme, they produce certain errors. In principle, such errors can be suppressed digitally, i.e., by applying single-qubit gates in an appropriate way and modifying algorithm itself. We, however, are not going to pursue this issue in the present paper.

III. TROTTERIZED EVOLUTION WITHIN MIXED ALROGITHMIC-ANALOG APPROACH

The feature of superconducting quantum processor architecture described in the preceding Section can be exploited to simulate physical systems in a nonstandard way. The idea is to use the internal physics of the quantum chip and apply it to modelling a Trotterized evolution of quantum systems, described by Hamiltonians with interactions, which can be reduced digitally to ZZ interaction discussed above. In particular, many spin Hamiltonians contain a

part of nearest-neighbour spin ZZ interaction (or XX interactions or combination of XX, YY and ZZ terms), and so the evolution generated by this part of Hamiltonian can be transferred to physics of the quantum processor. This approach can be applied to although specific but a wide class of problems: it is possible to use it to simulate dynamics of spin models such as Ising and Heisenberg models with arbitrary single spin terms of the Hamiltonian. A change of the basis is needed in order to simulate XX, YY, or ZX interaction, which is possible due to the individual control of qubits (single-qubit gates). It is also possible to apply this approach to construct entangled states naturally and then use those states in variational algorithms.

In order to illustrate our idea, we focus on the most straightforward example – simulation of spin clusters described by transverse-field Ising model with Hamiltonian

$$H = - \sum_j h_j \sigma_j^x - \sum_{\langle ij \rangle} J_{ij} \sigma_i^z \sigma_j^z, \quad (1)$$

where h_j are spin local fields and J_{ij} are interaction constants. This model requires to use only single-qubit gates to simulate the effect of terms $h_j \sigma_j^x$ since ZZ part of the Hamiltonian can be accounted for directly, i.e., by coupling between qubits of the quantum processor. It is worth noticing that in our experiments we used a trivial encoding, which means every spin is represented by a single qubit.

Let us stress that the actual topology of the quantum processor dictates the topology of the spin system we can simulate in such a mixed algorithmic-analog manner (at least, in a straightforward version we here implement). Moreover, existing ratios between values of J_{ij}^{phys} of the processor fix corresponding ratios between J_{ij} of the simulated spin system. Nevertheless, parameters h_j of the simulated system can be arbitrary thanks to the flexibility of digital (algorithmic) part of our mixed scheme.

To illustrate our ideas, we perform several experiments for two different physical setups. In particular, the first experiment deals with the dynamics of a transverse field Ising model for just two spins as a toy model. Every spin then is represented as a qubit of the quantum processor, and the Trotterized evolution is realized using both approaches. The first one is based on embedded ZZ interaction, while the second one is a standard digital approach based on two-qubit gates.

In order to trace free evolution of the system it is possible to use Trotter decomposition of evolution operator, which allows splitting an evolution operator for a full Hamiltonian consisting of non-commuting operators into a certain sequence of evolution operators for individual contributions. The simplest version of this decomposition for the Hamiltonian $H = H_A + H_B$ is

$$e^{-it(H_A+H_B)} \approx (e^{-iH_A \frac{t}{n}} e^{-iH_B \frac{t}{n}})^n, \quad (2)$$

which in $n \rightarrow \infty$ limit becomes exact. For transverse field Ising Hamiltonian, an appropriate splitting of the full Hamiltonian is

$$H_A = - \sum_j h_j \sigma_j^x, \quad (3)$$

$$H_B = - \sum_{\langle ij \rangle} J_{ij} \sigma_i^z \sigma_j^z, \quad (4)$$

where the latter term corresponds to ZZ interaction between qubits. Notations h_j , J_{ij} , and t refer to the system we wish to simulate (i.e., not to the actual parameters if the quantum processor). The ratios between J_{ij} and constants of ZZ interactions J_{ij}^{phys} of qubits of the chip must be the same, although the absolute values for the two sets of these quantities can be of course different.

In terms of quantum schemes, every two-qubit ZZ-rotation operator within the Trotterized evolution can be accomplished without actual application of any quantum gate and just waiting for some time instead, as depicted schematically in Fig. 1. Now let us determine this physical waiting time t^{phys} . Obviously, it is given by the relation $J_{ij} t = J_{ij}^{phys} t^{phys}$, so the controlling dimensionless parameters are $J_{ij}^{phys} t^{phys}$ sometimes referred to as Ising times. To implement such a time delay one needs to incorporate a particular number of identity gates I into the circuit. This number denoted as M can be calculated from a simple relation $M = t^{phys}/T_I$, where T_I is a physical time of the identity gate (in IBM Q machines, $T_I \approx 100$ ns and it also can vary from chip to chip). The technique can be incorporated into each Trotter step for the evolution operator, as described in Appendix A in a more detail.

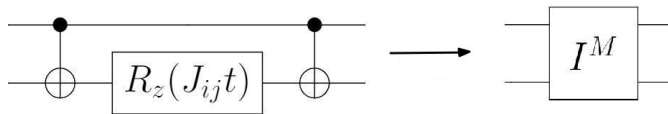


Figure 1: The evolution operator $\exp(-iJ_{ij}t\sigma_i^z\sigma_j^z)$ represented digitally in the standard way via CNOT gates (left picture) is replaced by the sequence of M identity gates I (right picture). In the latter case ZZ interaction between qubits of the processor produces the same effect (see in the text).

IV. MAIN RESULTS

A. Toy model: two spins

For the case of two qubits of quantum processor our approach is able to correctly reproduce dynamics of transverse field Ising system for initial basis states (e.g. $|00\rangle$ and $|11\rangle$) much better compared to the standard digital approach based on CNOT gates. The particular topology for the part of the IBM QX14 processor, used in calculation, is shown in Fig. 2, where qubits Q0 and Q1 were utilized for this simulation. Numbers placed between qubits show corresponding values of J_{ij}^{phys} (in kilohertz). We used 6-step Trotter decomposition to study the dynamics of the two-qubit system, the number of Trotter steps was chosen through a comparison with exact solution of the Schrodinger equation – for six steps the mathematical Trotterization error is not so significant for the evolution time we consider. Notice that we do not pay so much attention to this error, since our aim is to analyze errors associated with the hardware imperfections. Thus, we change t^{phys} ; for each value of t^{phys} we divide it into six intervals and implement six Trotter steps. The maximum t^{phys} was around 50 microseconds, which nearly corresponds to both T_1 and T_2 for a chosen quantum processor – apparently, this is the main restriction of our approach. Maximum dimensionless Ising time $J_{01}t = J_{01}^{phys}t^{phys}$ in simulations was equal to approximately 2.5. Every spin is supposed to be subjected to homogeneous transverse field. Both parameters h_0 and h_1 are chosen to be equal to $2J_{01}$ that corresponds to the regime when ZZ interaction and transverse field are of nearly equal importance.

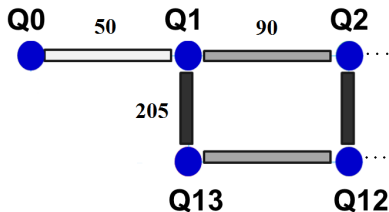


Figure 2: A schematic view of a part of IBM QX4 quantum processor utilized for simulation of the two-spin system (Q0 and Q1 are used). CNOT gates can be applied directly between those qubits which are connected by lines.

Qubits connected by these lines experience pairwise ZZ interaction of Ising type due to the presence of resonator they share. Numbers placed between qubits show corresponding values of coupling constants (in kilohertz).

Figure 3 shows that there is a good agreement between theoretical and experimental results, obtained using our approach, for the mean number of excited spins $\langle n(t) \rangle$ although there are some differences. The theoretical result is also based on 6-step Trotter decomposition, i.e., assumes an approximation of the same level. The agreement between the theory and the experiment based on the purely digital evolution is much more poor. We calculated several figures of merit to characterize further the quality of the simulation and the results are discussed in more detail in Appendix B.

It should be stressed that all actual connections of every chosen qubit to other qubits of the quantum processor should be taken into account in our simulations, because even if neighbouring qubits (Q2 and Q13 in this simulation) stay in ground states, they are still connected to qubits explicitly used in experiment (Q1) and influence their time evolution. Thus, in some sense, our simulation is performed for the four-spin cluster (Q0, Q1, Q2 and Q13), where two of the spins play a passive role, and not for the isolated couple of spins (Q0 and Q1).

The comparison of experimental data with theory is made by taking into account in the model the presence of these

surrounding qubits. Notice that in Subsection 4.4, we consider a dynamics of few-spin cluster in a more detail and show that couplings of qubits produce non-markovian dynamics.

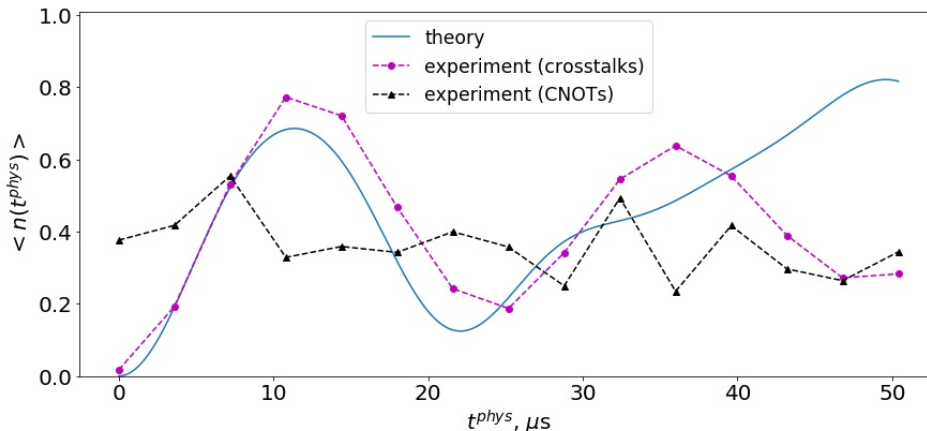


Figure 3: Dynamics of the mean excitation number for two-spin transverse field Ising cluster during the free evolution from the initial state $|00\rangle$. Shown are the results of the same approximation level (6 Trotter steps) obtained theoretically (blue color), experimentally within the mixed algorithmic-analog approach (magenta color) and experimentally within the purely algorithmic approach (black color). Physical time t^{phys} defines total time of algorithm execution within the mixed algorithmic-analog approach, which gives rise to ZZ interaction of qubits. For both theoretical result and the result of experimental implementation of purely algorithmic approach, t^{phys} must be mapped on time $t = J_{ij}^{phys} t^{phys} / J_{ij}$ of the simulated system.

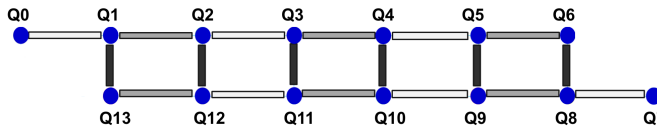


Figure 4: A topology of IBM QX14 quantum processor, which determines the connectivity map of 14-qubit cluster we simulate.

B. Dynamics of 14-spin cluster

In order to test our idea further we use again 14-qubit processor IBM QX14. A full connectivity map of this processor is provided in Fig. 4. We exploited all qubits of this quantum chip to model a temporal evolution of a spin cluster forming a ladder. We again assumed homogeneous field – all parameters h_j are the same and equal to the averaged over the cluster $2J_{ij}$.

In this experiment a Trotter decomposition of evolution operator for a 14 qubit spin system requires a huge number of two-qubit gates and thus a large error is expected, see, e.g., Ref. [38] dealing with purely algorithmic simulation of Ising model. The results presented in Fig. 5 were obtained using a 3-step Trotter decomposition of the evolution operator within three different cases: (i) using a unitary simulator of the quantum processor (theory), (ii) using our hybrid algorithmic-analog approach, and (iii) using a fully algorithmic (digital) approach.

From this figure we can clearly see, that a conventional algorithmic approach absolutely fails to reproduce a theoretically expected dynamics under already three Trotter steps. At the same time, if two-qubit gates are replaced with evolution of the system under crosstalks influence, then there is a good correspondence between theoretical and experimental results, although some constants J_{ij}^{phys} of the chip are as low as several tens of megahertz, so that the effect of decoherence must be significant on the time scale of $T_{1,2}$. Nevertheless, this approach for average over the cluster quantities works far better than the standard digital evolution. The reason is that every native two-qubit

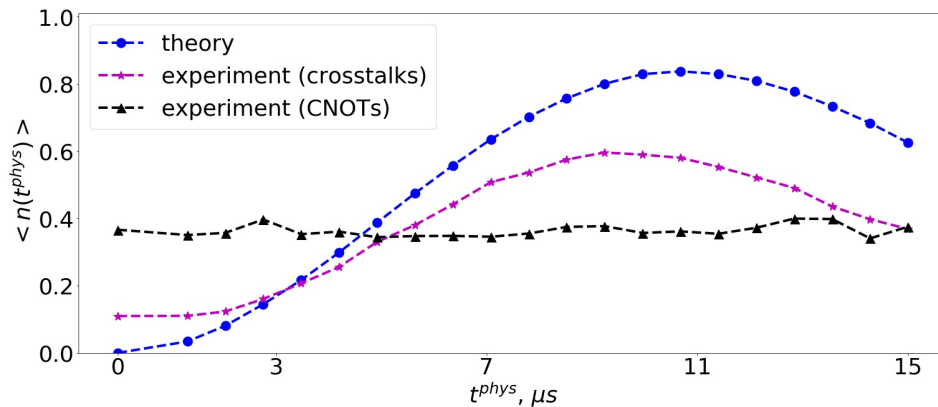


Figure 5: Dynamics of the mean excitation number for 14-spin transverse field Ising ladder during the free evolution from the initial state $|00\rangle$. Shown are the results of the same approximation level (3 Trotter steps) obtained theoretically (blue color), experimentally within the mixed algorithmic-analog approach (magenta color) and experimentally within the purely algorithmic approach (black color). Physical time t^{phys} defines total time of algorithm execution within the mixed algorithmic-analog approach, which gives rise to ZZ interaction of qubits. For both theoretical result and the result of experimental implementation of algorithmic approach, t^{phys} must be mapped on time $t = J_{ij}^{phys} t^{phys} / J_{ij}$ from the simulated model.

gate has an error of nearly 0.04 and to model a dynamics of 14 spin cluster, one needs to use dozens of such gates. Accumulation of errors of two-qubit gates is avoided within our approach and the main restriction is in the finiteness of $T_{1,2}$. Actually, within this time interval we can implement even larger number of Trotter steps than 3. In the next subsection we use 6 Trotter steps when simulating the effects of disorder on the dynamics. Increase of Trotter number decreases digitization error. Trotter number 3 was chosen because it already gives unacceptable results within the purely digital approach due to the errors of two-qubit gates.

Notice that, in principle, it is possible to extend the time of simulation beyond $T_{1,2}$ by using a dynamical decoupling within each "waiting" time interval. However, this issue is beyond of the scope of the present paper.

These result illustrate that mixed algorithmic-analog computation schemes are attractive for NISQ devices. Particularly, the ideas presented above highlight a perspective of using mixed algorithmic-analog approaches for simulation of many-body systems. We have used devices available from the cloud on the internet, for which we have no direct access and for which we can not really adjust parameters. We believe that it is possible to manufacture quantum devices and tune their controlling parameters in such a way as to make investigation of more interesting regimes possible within the mixed approach. For example, in Ref. [27] authors used quantum hardware with embedded interaction between qubits and investigated a phenomenon of many-body localization in an XY spin model without usage of Trotterization. The Trotterized evolution has an advantage which originates from the flexibility of digitization – the effect of various additional (tunable) terms of the modelled Hamiltonian not present in the actual interaction of qubits in the chip, can be emulated. The disadvantage of this strategy is associated with additional digitization errors.

C. Emulation of the effect of disorder

In this subsection, we emulate an effect of disorder on many body dynamics of 14-qubit spin cluster. Actually, crosstalks, used for our modelling, are already characterized by a sort of disorder in J_{ij}^{phys} . We introduced an additional disorder by incorporating into Hamiltonian (1) a set of terms $\epsilon_j \sigma_j^z$, where constants ϵ_j are random. We than consider a dynamics of 14-spin cluster from the state, in which half of the spins are in spin up states, while another half in spin down states, as shown in Fig. 6. In our simulations, we assume that values of ϵ_j are randomly chosen from a uniform distribution in the interval $[-2\bar{J}, 2\bar{J}]$, \bar{J} being an average interaction between all spins of the system.

Figure 7 shows both theoretical (obtained from the unitary simulator) and experimental data for the magnetization $2\langle\sigma^z\rangle$ of qubits of the chip as a function of time, when no additional disorder is introduced into the model. Figure

8 provides similar data, but in presence of the disorder – typical representative result for a particular realization of disorder is shown, but, in total, we have studied 10 realizations with IBM QX14 quantum processor. Numbering of qubits is the same as in Fig. 6. Trotter number in both experimental and theoretical approaches was 6. Typical digitization error is below 10 percent up to the simulation time $t^{phys} \approx 30$ microseconds, but then it grows. Still, this Trotter number is sufficient to see qualitatively correct picture of the actual evolution (full solution of time dependent Schrodinger equation).

From Figs. 7 and 8 we can see that an initial pattern of magnetization behaves more stable with time in the presence of disorder we introduced than in its absence. This means that the spread of correlation between qubits is being suppressed, which is consistent with our knowledge of localization phenomena. Although performing these experiments on the IBM QX14 quantum processor shows some discrepancies from unitary simulation, it still preserves the same qualitative behaviour. In the presence of disorder we can clearly see the stability of the magnetization pattern similar to the theoretical result. So we conclude that our strategy allows to witness a qualitative correspondence of theoretical and experimental results, which could be even better once we have control over interaction strength between qubits.

Let us stress that Trotterization provides a certain flexibility, which can be used in simulations. We now briefly discuss one example. As it was mentioned before, all parameters J_{ij}^{phys} are positive. If we somehow manage to change the signs of some of these constants, we may emulate a spin cluster in which some spin-spin interactions favor ferromagnetic ordering, while others support antiferromagnetic order. We suggest a trick associated with the spin flip which allows to emulate negative values of these constants. A sign change can be introduced via the basis change of the spin (qubit) system: $|0\rangle \rightarrow |1\rangle$. This is accomplished by the following transformation:

$$\sigma_j^z \rightarrow 1 - \sigma_j^z, \quad (5)$$

which inverts a sign of the constant J_{ij}^{phys} , provided only a single qubit of the couple (i, j) was flipped. The transformation gives rise to new single-spin terms of the form $J_{ij}\sigma_i^z$ in the Hamiltonian. They can be suppressed digitally by adding opposite terms in Hamiltonian (single-qubit rotations within each Trotter step). Having this in mind, we can choose randomly certain fraction of qubits of the processor and flip their states within our computation scheme, as described above. This effectively corresponds to the disordered spin cluster with both ferro and antiferromagnetic links.

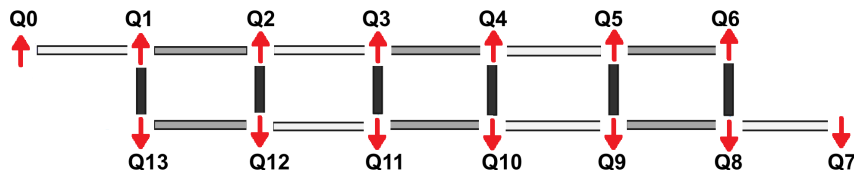


Figure 6: Initial states of the spin cluster. The free evolution of the system from this state is studied.

D. Nonmarkovian dynamics of qubits

As it was already mentioned in Subsection 4.1, a constant interqubit interaction is a source of a dynamics of qubit states even in absence of microwave pulses. Although this feature can be used in a positive way along the general idea of this paper, it can also influence in an uncontrollable way other calculations on the quantum processor. To illustrate this statement we considered a simple experiment of tracing dynamics of different quantum states for one chosen qubit of a quantum processor. If this qubit has connection to surrounding qubits (which serve as environment), the dynamics can be described using an open quantum system approach. Using this approach we address a relation between state of the environment and the observable dynamics of target qubit.

It is known that open quantum systems can roughly show two general types of dynamical behaviour, a markovian quantum evolution and a non-markovian quantum evolution. The first one is characterized by non-correlated envi-

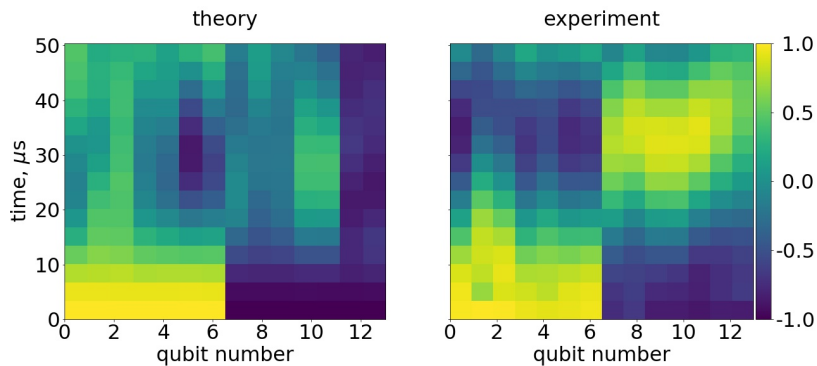


Figure 7: A pattern of magnetization, calculated on a unitary quantum simulator (left panel) and on IBM QX14 quantum processor (right panel) over time for a 14-spin cluster during the free evolution under the transverse field Ising Hamiltonian in the absence of disorder (6 Trotter steps).

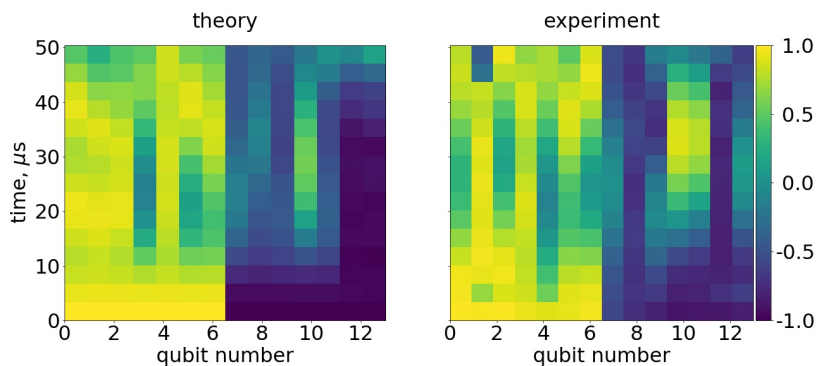


Figure 8: A pattern of magnetization, calculated on a unitary quantum simulator (left panel) and on IBM QX14 quantum processor (right panel) over time for a 14-qubit system during the free evolution under the transverse field Ising Hamiltonian in the presence of artificial disorder (6 Trotter steps).

ronment and one-way information flow between system and environment, while the second one is characterized by correlated environment and a backflow of information from environment into the system [34].

In order to find out if the dynamics of a system under the scope is one or another, we can use a trace distance metric, which is capable to show how distinct two quantum states are. This measure is able to characterize the behaviour of open system dynamics: if a trace distance between two initially distinct quantum states decays over time monotonically, then the system shows markovian dynamics, and if it decays non monotonically and has periods of growth, then the dynamics is non-markovian ([35], [36]). To reveal those effect clearly one should use states which are maximally distinct at the initial moment of the experiment [37].

In our experiments, we used 5-qubit quantum processor IBM QX4 shown schematically in Fig.9. Qubit Q_0 was chosen as a target one, and consequently Q_1 and Q_2 qubits were treated as an environment. Within a ZZ-interaction model one can obtain simple expressions for the trace distance between qubit states over time for different states of surrounding qubits (see Appendix C for details):

$$D(t) = 1 \quad (6)$$

for the case of a separable environment state $|00\rangle$, while

$$D(t) = |\cos[2(J_{01} \pm J_{02})t]| \quad (7)$$

for Bell states $|\Phi_{\pm}\rangle$ and $|\Psi_{\pm}\rangle$ of the environment, where $+$ ($-$) corresponds for $|\Phi_{\pm}\rangle$ ($|\Psi_{\pm}\rangle$).

The experiment we performed is as follows. The chosen qubit has been prepared in pairs of maximally distinct initial states (those states were $|0\rangle$ and $|1\rangle$, $|+\rangle$ and $|-\rangle$) and its dynamic was studied for different states of surrounding qubits

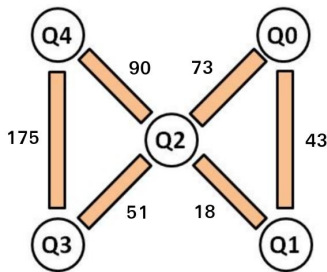


Figure 9: A schematic view of IBM QX4 quantum processor. CNOT gates can be applied directly between those qubits which are connected by orange lines. Qubits connected by these lines experience pairwise ZZ interaction of Ising type due to the presence of resonator they share. Numbers placed between qubits show corresponding values of coupling constants (in kilohertz).

(those are separable ground state $|00\rangle$ and maximally-entangled Bell states). Such an experiment should reveal any nontrivial influence of surrounding processor qubits on the target one. If we see trace distance changes monotonically, then we know that whatever the surrounding qubits are, they do not influence evolution of any prepared state on the target qubit. If we see trace distance changes nonmonotonically (say, it has periods of growth), then evolution of a target qubit depends on the state of its surrounding qubits. The results of the experiment are shown in Fig. 9, where data obtained through experiment on a quantum processor IBM QX4 are compared with exact calculation of qubit states dynamics. In this experiment the target qubit was prepared in states $|+\rangle$ and $|-\rangle$, then in both cases for every time point there was obtained a density matrix through quantum state tomography and then the trace distance was calculated. The surrounding qubits were prepared in maximally entangled Bell state $|\Phi_+\rangle$. We can see, that trace distance has a strongly nonmonotonical behaviour. Comparison with ZZ interaction picture without taking decoherence into account shows good qualitative correspondence between theory and experimental results. No fitting parameter was used. This means, that constant coupling between qubits leads to non-markovian dynamics of target qubit states. We also conducted other experiments, where target qubit was prepared in one of the Z basis states for both separable and maximally entangled surroundings as well as superpositional target qubit state with separable surrounding qubit states. Those last experiments showed monotonically changing trace distance.

Through these experiments we observed, that a state of surrounding qubits has a strong influence on the dynamics of superpositional states of the target qubit. This observation shows that constant interaction between qubits, which is present in a superconducting quantum processors with fixed frequency, serves as an additional limitation to quantum computation procedures. From Fig. 10 we can see, that the time needed for two initial quantum states to become indistinguishable under the influence of this interaction is far less than characteristic coherency times. This interaction adds additional correlation between quantum errors, both temporal and spatial. This fact should be kept in mind while doing computations on this kind of quantum processors. It is also of great importance for future error correction works with quantum processors since this means that the presence of a residual interaction between qubits leads to correlated errors, which makes an implementation of fault tolerant quantum computing more challenging.

V. CONCLUSIONS

In this paper we have revealed an unexpected opportunity to use residual (parasitic) couplings between qubits, which are present in superconducting quantum processors based on fixed frequency qubits, to simulate dynamics of many body spin systems within a mixed algorithmic-analog strategy based on Trotterization of evolution operator.

We provided results of several experiments with quantum processors of IBM Quantum Experience aimed to test this idea and showed that our approach demonstrates advantages compared to a conventional digital quantum computation with the same quantum processors (at least, for certain problems). In particular, we showed that this approach allows to obtain good results for the dynamics of spin clusters with up to 14 spins (number of qubits in the available quantum processor), while similar calculation with the same processor using standard two-qubit gates leads to unacceptable low accuracy due to accumulation of gates errors. Furthermore, we have shown that even with modest opportunities to control parameters of the quantum hardware it is still possible to model effects of disorder thanks to the flexibility of

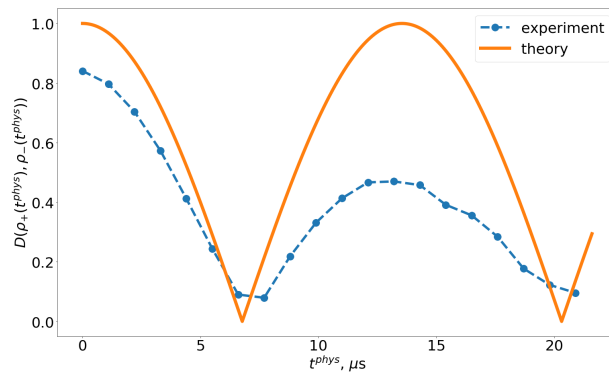


Figure 10: A plot of trace distance over time for a Q_0 qubit, surrounded by Q_1 and Q_2 qubits. Trace distance was calculated for data from two experiments: qubit Q_0 was prepared in states $|+\rangle$ and $|-\rangle$ and its temporal evolution was obtained by doing quantum state tomography for every time point. The surrounding qubits Q_1 and Q_2 were prepared in a maximally entangled state $|\Phi_+\rangle$. Orange curve corresponds to exact calculation of trace distance dynamics and blue curve corresponds to calculation on a quantum processor.

Trotterization allowing for the incorporation of artificial randomness. From these results we point out on a perspective of using digital-analog quantum computation strategy within NISQ technology.

We also showed that the residual coupling between qubits gives rise to highly non-markovian dynamics of qubits and argued that this fact must be taken into account in implementation of error-correction codes.

Acknowledgments. – We acknowledge use of the IBM Quantum Experience for this work. The viewpoints expressed are those of the authors and do not reflect the official policy or position of IBM or the IBM Quantum Experience team.

-
- [1] Yu. Manin, *Computable and Noncomputable*, Russian: Sov. Radio, 128 (1980).
 - [2] R. Feynmann, *Simulating physics with computers*, *Int. J. Theor. Phys.* **21**, 467 (1982).
 - [3] P. W. Shor, *Polynomial-Time Algorithms for Prime Factorization and Discrete Logarithms on a Quantum Computer*, *SIAM Review* **26**, 1484 (1996).
 - [4] A. W. Harrow, A. Hassidim and S. Lloyd, *Quantum Algorithms for linear systems of equations*, *Phys. Rev. Lett.* **103**, 150502 (2009)
 - [5] S. Lloyd, M. Mohseni and P. Rebentrost, *Quantum Principal Component Analysis*, *Nat. Phys.* **10**, 631 (2014).
 - [6] C. Neill, P. Roushan, K. Kechedzhi, S. Boixo, S. V. Isakov, V. Smelyanskiy, R. Barends, B. Burkett, Y. Chen, Z. Chen, B. Chiaro, A. Dunsworth, A. Fowler, B. Foxen, R. Graff, E. Jeffrey, J. Kelly, E. Lucero, A. Megrant, J. Mutus, M. Neeley, C. Quintana, D. Sank, A. Vainsencher, J. Wenner, T. C. White, H. Neven, and J. M. Martinis, *A blueprint for demonstrating quantum supremacy with superconducting qubits*, *Science* **360**, 195 (2018).
 - [7] <https://www.research.ibm.com/ibm-q/>
 - [8] <https://www.rigetti.com/>
 - [9] <https://ionq.co/>
 - [10] J. Preskill, *Quantum Computing in the NISQ era and beyond*, *Quantum* **2**, 79 (2018).
 - [11] M. A. Nielsen and I. L. Chuang, *Quantum Computation and Quantum Information* (2nd ed.). Cambridge: Cambridge University, (2010).
 - [12] S. J. Devitt, W. J. Munro and K. Nemoto, *Quantum error correction for beginners*, *Rep. Prog. Phys.* **76**, 076001 (2013).
 - [13] K. Temme, S. Bravyi, J. M. Gambetta, *Error mitigation for short-depth quantum circuits*, *Phys. Rev. Lett.* **119**, 180509 (2017).
 - [14] Y. Li and S. C. Benjamin, *Efficient Variational Quantum Simulator Incorporating Active Error Minimization*, *Phys. Rev. X* **7**, 021050 (2017).
 - [15] J. R. McClean, M. E. Kimchi-Schwartz, Jonathan Carter, and W. A. de Jong, *Hybrid quantum-classical hierarchy for mitigation of decoherence and determination of excited states*, *Phys. Rev. A* **95**, 042308 (2017).
 - [16] S. Endo, S. C. Benjamin, Y. Li, *Practical Quantum Error Mitigation for Near-Future Applications*, *Phys. Rev. X* **8**, 031027 (2018).

- [17] A. Kandala, A. Mezzacapo, K. Temme, M. Takita, M. Brink, J. M. Chow, and J. M. Gambetta, Hardware-efficient Variational Quantum Eigensolver for Small Molecules and Quantum Magnets, *Nature* **549**, 242 (2017).
- [18] E. F. Dumitrescu, A. J. McCaskey, G. Hagen, G. R. Jansen, T. D. Morris, T. Papenbrock, R. C. Pooser, D. J. Dean, and P. Lougovski, Cloud Quantum Computing of an Atomic Nucleus, *Phys. Rev. Lett.* **120**, 210501 (2018).
- [19] S. C. Benjamin and S. Bose, Quantum computing in arrays coupled by always-on interactions, *Phys. Rev A* **70**, 032314 (2004).
- [20] E. Farhi, J. Goldstone, and S. Gutmann, A Quantum Approximate Optimization Algorithm, arXiv:1411.4028 (2014).
- [21] J. R. McClean, J. Romero, R. Babbush, and A. Aspuru-Guzik, The theory of variational hybrid quantum-classical algorithms, *New J. Phys.* **18** 023023 (2015).
- [22] A. Parra-Rodriguez, P. Lougovski, L. Lamata, E. Solano, and M. Sanz, Digital-Analog Quantum Computation, arXiv: 1812.03637 (2018).
- [23] K. Xu, J.-J. Chen, Y. Zeng, Y.-R. Zhang, C. Song, W. Liu, Q. Guo, P. Zhang, D. Xu, H. Deng, K. Huang, H. Wang, X. Zhu, D. Zheng, and H. Fan, Emulating Many-Body Localization with a Superconducting Quantum Processor, *Phys. Rev. Lett.* **120**, 050507 (2018).
- [24] A. Smith, M. S. Kim, F. Pollmann, and J. Knolle, Simulating quantum many-body dynamics on a current digital quantum computer, arXiv:1906.06343 (2019).
- [25] J. Smith, A. Lee, P. Richerme, B. Neyenhuis, P. W. Hess, P. Hauke, M. Heyl, D. A. Huse, and C. Monroe, Many-body localization in a quantum simulator with programmable random disorder, *Nat. Phys.* **12**, 907 (2016).
- [26] P. Jurcevic, B. P. Lanyon, P. Hauke, C. Hempel, P. Zoller, R. Blatt, and C. F. Roos, Observation of entanglement propagation in a quantum many-body system, *Nature* **511**, 202 (2014).
- [27] A. Martin, L. Lamata, E. Solano, and M. Sanz, Digital-analog quantum algorithms for the quantum Fourier transform, arXiv: 1906.07635v1 (2019).
- [28] I. M. Georgescu, S. Ashhab, and F. Nori, Quantum simulation, *Rev. Mod. Phys.* **86**, 153 (2014).
- [29] J. M. Gambetta, Control of Superconducting Qubits, 44th IFF Spring School lecture notes (2013).
- [30] E. Magesan, J. M. Gambetta, Effective Hamiltonian models of the cross-resonance gate, arXiv:1804.04073 (2018).
- [31] <https://github.com/Qiskit/ibmq-device-information/tree/master/backends>
- [32] D. A. Lidar and T. A. Brun, *Quantum Error Correction*, Cambridge University Press (2013).
- [33] D. V. Babukhin, A. A. Zhukov, and W. V. Pogosov, Nondestructive classification of quantum states using an algorithmic quantum computer, arXiv:1909.05596 (2019).
- [34] H. P. Breuer, E. M. Laine, J. Piilo, and B. Vacchini, Non-Markovian dynamics in open quantum systems, *Rev. Mod. Phys.* **88**, 021002 (2016).
- [35] H. P. Breuer, E. M. Laine, and J. Piilo, Measure for the Degree of Non-Markovian Behavior of Quantum Processes in Open Systems, *Phys. Rev. Lett.* **103**, 210401 (2009).
- [36] E. M. Laine, J. Piilo, and H. P. Breuer, Measure for the Non-Markovianity of Quantum Processes, *Phys. Rev. A* **81**, 062115 (2010).
- [37] S. Wissmann, A. Karlsson, E. M. Laine, J. Piilo, and H. P. Breuer, Optimal state pairs for non-Markovian quantum dynamics, *Phys. Rev. A* **86**, 062108 (2012).
- [38] A. A. Zhukov, S. V. Remizov, W. V. Pogosov, and Yu. E. Lozovik, Algorithmic simulation of far-from-equilibrium dynamics using quantum computer, *Quantum Inf. Process.* **17**, 223 (2018).

Appendix A

Each Trotter step for the evolution operator corresponding to two spins i, j and Hamiltonian (1) can be represented in terms of quantum schemes shown in Fig. 11.

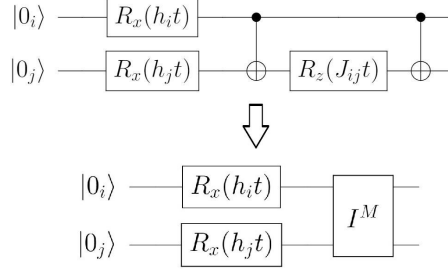


Figure 11: Single Trotter step for a couple of spins described by the transverse field Ising model. The upper picture represents a standard digital decomposition into quantum gates. The lower picture represents the same subroutine based on the ZZ interaction of the qubits of the quantum chip.

Appendix B

To quantify results from the section 4.1 we use the several figures of merit. We analyze l_1 metric defined as

$$l_1(t) = |X^{exp}(t) - X^{theory}(t)|, \quad (\text{B1})$$

where $X^{exp}(t)$ and $X^{theory}(t)$ are experimental and theoretical observable values at moment t correspondingly. The resulting plot is provided in Fig. 12, which shows better accuracy of our mixed approach compared to the standard digital approach. As the physical simulation time approaches T_1 and T_2 , the agreement between the theory and the results of our approach also becomes unsatisfactory.

We also perform a frequency analysis of $\langle n(t) \rangle$, which is presented in Fig. 13. The Fourier components of $\langle n(t) \rangle$ are

$$n(\omega_k) = \sum_{m=0}^{n-1} \tilde{n}(t_m) \exp\left(-2\pi i \frac{t_m \omega_k}{n}\right), \quad k = 0, \dots, n-1, \quad (\text{B2})$$

where $\tilde{n}(t_m)$ are normalized values of $\langle n(t) \rangle$:

$$\tilde{n}(t_m) = \frac{n(t_m)}{\max_{t_m} n(t_m)} \quad (\text{B3})$$

where t_m is a moment of evolution time of the excitation measurement. Figure 13 illustrates that noisy two-qubit gates increase the zero frequency component, i.e. effectively flatten time dependence of $\langle n(t) \rangle$ besides changing its time variation character. We have already seen such a tendency towards flattening of various quantities evaluated using noisy quantum hardware as functions of controlling parameters [33].

Appendix C

We elaborate on derivation of trace distance expressions for our experimental setup. First, we consider a system of three qubits, one being a target and two being an environment. We suppose that the interaction between those qubits is due to ZZ-interaction, which is described with the following hamiltonian:

$$H_{zz} = J_{01}^{phys} \sigma_0^z \sigma_1^z + J_{02}^{phys} \sigma_0^z \sigma_2^z + J_{12}^{phys} \sigma_1^z \sigma_2^z. \quad (\text{C1})$$

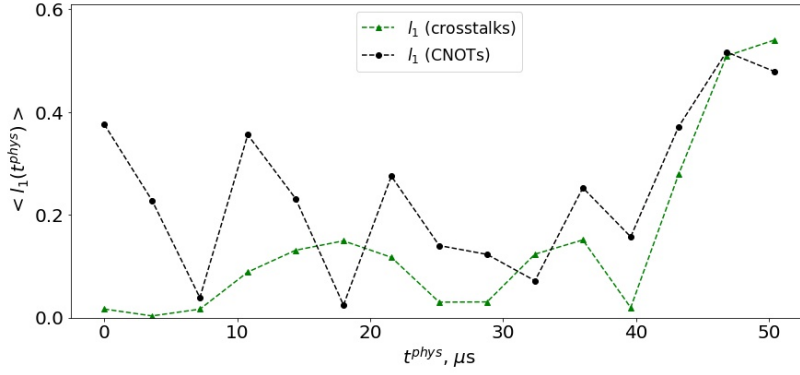


Figure 12: Resulting plots of averaged over two qubits l_1 metric for two-qubit initial state $|00\rangle$ as a function of time during the free evolution. The experimental results within both the mixed algorithmic-analog approach and within the purely algorithmic approach are shown.

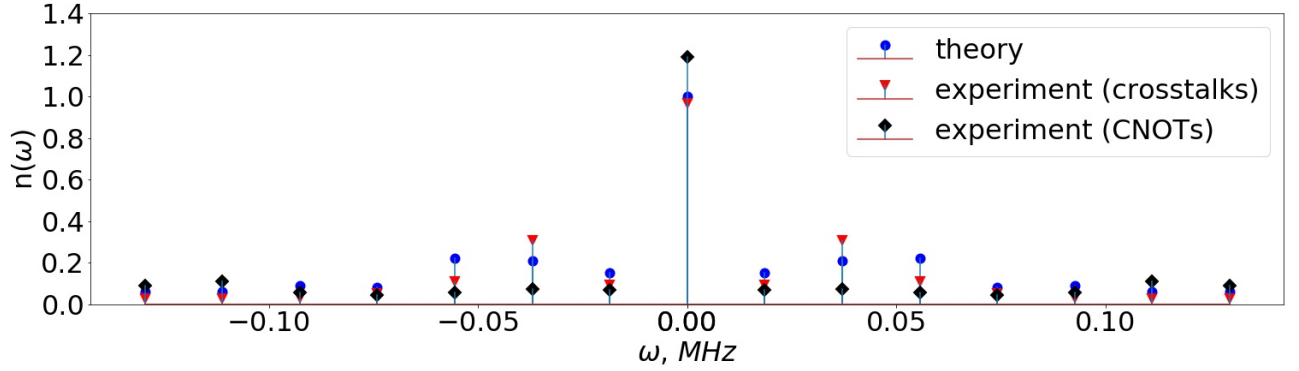


Figure 13: Fourier components of the mean excitation number as a function of time.

The initial state of this system for the environment state of the general form reads:

$$|\Psi(0)\rangle = |S\rangle |E\rangle \quad (\text{C2})$$

where $S = 0, 1, +$ or $-$ and environment state has the form:

$$|E\rangle = \alpha |00\rangle + \beta |01\rangle + \gamma |10\rangle + \delta |11\rangle \quad (\text{C3})$$

After evolution under ZZ hamiltonian the system of one qubit can end up being partially entangled with environment and generation of this entanglement is in essence an information flow out of the system. In operational language this means that if two initial state were clearly distinct at the beginning, then those states will be less and less distinct with the flow of time. If the informational flow is one way, then after some time two initial states will be completely indistinguishable. But if the system-environment dynamics allows for information to flow back into the system, then distinguishability of two states will rise during some periods of time. Both cases can be captured by analyzing a measure of distinction between two quantum states, which is a trace distance defined as [11]:

$$D = \frac{1}{2} \text{Tr} \sqrt{(\rho_1 - \rho_2)^\dagger (\rho_1 - \rho_2)} \quad (\text{C4})$$

where ρ_1, ρ_2 are two states of a system.

After straightforward calculation one can obtain density matrices for different initial target qubit system states after evolving for time t^{phys} under H_{zz} :

$$\rho_0(0) = \begin{pmatrix} 1 & 0 \\ 0 & 0 \end{pmatrix} \longrightarrow \rho_0(t^{phys}) = \begin{pmatrix} 1 & 0 \\ 0 & 0 \end{pmatrix},$$

$$\rho_1(0) = \begin{pmatrix} 0 & 0 \\ 0 & 1 \end{pmatrix} \longrightarrow \rho_1(t^{phys}) = \begin{pmatrix} 0 & 0 \\ 0 & 1 \end{pmatrix},$$

$$\rho_{\pm}(0) = \begin{pmatrix} \frac{1}{2} & \pm\frac{1}{2} \\ \pm\frac{1}{2} & \frac{1}{2} \end{pmatrix} \longrightarrow \rho_{\pm}(t^{phys}) = \begin{pmatrix} \frac{1}{2} & \pm B(t^{phys}) \\ \pm B^*(t^{phys}) & \frac{1}{2} \end{pmatrix},$$

where

$$B(t^{phys}) = e^{-i\omega_0 t^{phys}} \left(\frac{|\alpha|^2}{2} e^{-2i(\tau_{01} + \tau_{02})} + \frac{|\beta|^2}{2} e^{-2i(\tau_{01} - \tau_{02})} + \frac{|\gamma|^2}{2} e^{2i(\tau_{01} - \tau_{02})} + \frac{|\delta|^2}{2} e^{2i(\tau_{01} + \tau_{02})} \right), \quad (\text{C5})$$

where $\tau_{ij} = J_{ij}^{phys} t^{phys}$. It is clear that for initial quantum states with a trivial relative phase in Z-basis there is no influence of any kind from surrounding qubits through ZZ-interaction. On the other side, when initial state has a non-trivial quantum phase, there is a strong influence on target qubit dynamics. For trace distance we obtain:

$$D = 2\sqrt{BB^*}, \quad (\text{C6})$$

where

$$BB^* = \frac{|\alpha|^2 + |\beta|^2 + |\gamma|^2 + |\delta|^2}{4} + \frac{|\alpha|^2|\beta|^2 + |\gamma|^2|\delta|^2}{2} \cos \tau_{02} + \frac{|\alpha|^2|\gamma|^2 + |\beta|^2|\delta|^2}{2} \cos \tau_{01} + \frac{|\alpha|^2|\delta|^2}{2} \cos(\tau_{01} + \tau_{02}) + \frac{|\delta|^2|\gamma|^2}{2} \cos(\tau_{01} - \tau_{02}).$$

. For particular case of environment states ($\alpha = \delta = \frac{1}{\sqrt{2}}, \beta = \gamma = 0$ for $|\Phi_{\pm}\rangle$ or $\alpha = \delta = 0, \beta = \gamma = \frac{1}{\sqrt{2}}$ for $|\Psi_{\pm}\rangle$) we obtain Eq. (7) from the main text.